The Carboxyl Terminal Residues 220–283 Are Not Required for Voltage Gating of a Chimeric Connexin32 Hemichannel

Taekyung Kwon,[†] Terry L. Dowd,[‡] and Thaddeus A. Bargiello[†*]
[†]Dominic P. Purpura Department of Neuroscience, Albert Einstein College of Medicine, Bronx, New York; and [‡]Department of Chemistry, Brooklyn College of the City University of New York, Brooklyn, New York

ABSTRACT Connexin hemichannels display two distinct forms of voltage-dependent gating, corresponding to the operation of V_j- or fast gates and loop- or slow gates. The carboxyl terminus (CT) of connexin 32 has been reported to be required for the operation of the V_j (fast) gates, but this conclusion was inferred from the loss of a fast kinetic component in macroscopic currents of CT-truncated intercellular channels elicited by transjunctional voltage. Such inferences are complicated by presence of both fast and slow gates in each hemichannel and the serial head-to-head arrangement of these gates in the intercellular channel. Examination of voltage gating in undocked hemichannels and V_j gate polarity reversal by a negative charge substitution (N2E) in the amino terminal domain allow unequivocal separation of the two gating processes in a Cx32 chimera (Cx32*43E1). This chimera expresses currents as an undocked hemichannel in *Xenopus* oocytes and provides a model system to study the molecular determinants and mechanisms of Cx32 voltage gating. Here, we demonstrate that both V_j- and loop gates are operational in a truncation mutation that removes all but the first four CT residues ($ACAR^{219}$) of the Cx32*43E1 hemichannel. We conclude that an operational Cx32 V_j (fast) gate does not require CT residues 220–283, as reported previously by others.

INTRODUCTION

All connexin hemichannels, whether docked to an apposed hemichannel to form an intercellular channel (gap junction) or unapposed in the plasma membrane (undocked hemichannel), display two distinct forms of voltage-dependent gating; termed V_j- or fast gating and loop- or slow gating. The two gating processes were initially defined by the form of gating transitions observed in single-channel records of an undocked Cx46 hemichannel (1). V_j- or fast gating corresponds to transitions between the open and distinct subconductance (residual) states that cannot be further resolved within the time resolution of patch-clamp recordings, hence the term fast gating. In contrast, loop- or slow gating corresponds to a complex gating transition that connects an open and a fully closed state through a series of intermediate metastable conformations, giving the appearance of a slow transition characterized by time constants in the order of tens of milliseconds in single-channel records (1–4). In macroscopic recordings, the time constant of V_j gating is faster and more sensitive to voltage than loop gating, at least for some connexin channels (4).

The two processes can also be distinguished by their gating polarity. In all undocked connexin hemichannels examined to date, loop gate closure is favored with membrane hyperpolarization, whereas the polarity of V_j (fast) gate closure can be favored at either depolarizing or hyperpolarizing membrane potentials in a connexin-specific manner. For example, V_j (fast) gate closure of Cx26 and Cx46 undocked hemichannels is favored at inside positive potentials (depolarization from 0 mV) (1,2,5–7), whereas that of chimeric Cx32 (Cx32*43E1) and Cx43 hemichannels is favored at inside negative potentials (hyperpolarization from 0 mV) (4,5,7–10).

In intercellular channels, both gating processes are sensitive to transjunctional voltage (V_j), which is defined as the difference in the potential of the cytoplasms of the two coupled cells (see Fig. 1 in Bukauskas and Verselis (4)). It is well established that the sensitivity of intercellular channels to transjunctional voltage is an intrinsic hemichannel property, in that each hemichannel contains both sets of voltage sensors and gates that function autonomously, but not necessarily independently when two hemichannels are paired to form an intercellular channel. Because of the head-to-head arrangement of the two hemichannels, the voltage sensors and gates are oriented oppositely in each hemichannel. Thus, polarizations that favor closure of a given gate in one hemichannel will favor opening of this gate in the apposed hemichannel (4,5). This feature may complicate the study of the operation of the two gates in hemichannels when they are paired to form intercellular channels. The polarity of the closure of the V_j (fast) gates can in some cases be inferred by comparisons of the conductance-voltage relations of intercellular channels in homotypic and heterotypic pairing configurations because of the greater sensitivity of V_j gates to transjunctional voltage (3,5). For example, in Cx32/Cx26 heterotypic intercellular channels, closure of the V_j (fast) gates is favored when the Cx32 side of the intercellular channel experiences a relatively negative transjunctional voltage, whereas closure of the Cx26 V_j (fast) gate is favored at relatively positive transjunctional potentials (5). Historically, operation of the V_j (fast) gates was termed "V_j gating", because the presence of two gating mechanisms that are both sensitive to

Submitted June 3, 2013, and accepted for publication August 12, 2013.

*Correspondence: ted.bargiello@einstein.yu.edu

Editor: Claudia Steinem.

0006-3495/13/09/1376/7 $2.00

http://dx.doi.org/10.1016/j.bpj.2013.08.015

transjunctional voltage had not yet been established. In this article, we use the term "V_j gating" to describe the operation of the V_j (fast) gates and "loop gating" to describe the operation of loop (slow) gates.

The opposite polarity of the V_j (fast) gates in Cx32 and Cx26 hemichannels maps to a difference in the charge of the second amino acid in the N-terminal domain (NT, residues 1–22). The negative charge, D2, in Cx26 results in positive gating polarity, i.e., closure of the gate at positive potentials in undocked hemichannels and closure of the gate in the hemichannel that experiences a relatively positive transjunctional voltage in intercellular channels. The neutral residue, N2, in Cx32 results in negative gating polarity (5). The substitution of a negative charge at the second, fourth, or fifth residues in Cx32 and its chimera Cx32*43E1 reverses gating polarity from closure at inside negative potentials to closure at inside positive potentials, as demonstrated in both macroscopic and single-channel recordings (5,7,8,11,12). Neutral and positive charge substitutions of residue D2 reverse the Cx26 V_j gating polarity (5). Furthermore, heteromeric undocked Cx32*43E1 hemichannels containing a single-polarity reversing subunit display bipolar V_j gating in single-channel recordings (12). Together, these results suggest that N-termini of Cx26 and Cx32 hemichannels contain at least a portion of the V_j gate voltage sensor and that closure results from conformational changes in individual connexin subunits rather than by a cooperative (concerted) mechanism involving all six hemichannel subunits (12).

Two different molecular mechanisms have been proposed to explain V_j (fast) gating (reviewed in Bargiello et al. (3) and González et al. (13)):

The first mechanism, termed the "plug" model, was proposed by Oshima et al (14) and Maeda et al. (15). In this model, the permeability barrier is formed solely by changing the position of the N-terminus of Cx26 hemichannels within the channel vestibule.

The second mechanism, termed the "particle-receptor" or "ball-and-chain" model, was proposed for V_j (fast) gating of Cx43 and Cx40 hemichannels. This model proposes that an interaction between a region in the C-terminus, or CT (which is the particle, consisting of residues 265–276 in Cx43), and a region in the cytoplasmic loop, or L2 (which is the receptor, consisting of residues 119–144 in Cx43), mediates the fast gating process. Overall, the particle-receptor voltage gating model parallels that proposed to explain pH gating of Cx43 by Lewandowski et al. (16), in that both involve the same protein domains. Although it should be noted that at the single-channel level, pH gating involves slow transitions like those observed in voltage-dependent slow gating and not fast gating. The relation between slow gating events elicited by pH and voltage has not been established, although it has been proposed that they may arise by the same molecular mechanism (4). Notably however, pH gating of Cx46 undocked hemichannels appears to differ from that reported for Cx43 gap junctions (17).

The Cx43 particle-receptor model is based on the following observations:

1. Fast gating is lost in a Cx43-CT truncation at residue 258 (18,19).
2. Addition of EGFP to the C-terminus of Cx43 appears to abolish fast gating transitions in single-channel recordings (4,10).
3. Fast gating is restored by addition of the Cx43-CT as a separate protein fragment (18).
4. Fast gating is abolished by addition of the L2 peptide (20) to the wild-type channel, presumably by binding to the intact CT.
5. Fast gating is attenuated by mutation of residue H142 located within the L2 region (21).

Furthermore, molecular interactions between regions of the CT and L2 segment were identified by NMR studies of Cx43 and Cx40 peptides (21–24).

Revilla et al. (19) reported that truncations of Cx32 at residue 220 (but see Materials and Methods) altered the time constants of channel closure reducing a fast component of voltage gating in macroscopic recordings of intercellular Cx32 channels elicited by transjunctional voltage. They interpreted the kinetic change to indicate the loss of the V_j (fast) gate and concluded that the CT of Cx32, like that of Cx43, was critical to the expression of V_j (fast) gating. In their interpretation, the remaining current relaxation was ascribed to closure of the loop (slow) gates, but the loss of V_j (fast) gates and persistence loop (slow) gates were not confirmed by single-channel recordings.

Here, we reexamine this conclusion by examining voltage-dependent gating of a chimeric hemichannel Cx32*43E1, in which the first extracellular loop of Cx32 residues 41–70 is replaced with that of Cx43 and the CT is truncated to residue 219 by insertion of a stop codon in place of residue 220. Our past studies have demonstrated that the chimera is a good model system for studying the mechanisms of Cx32 voltage gating (reviewed in Bargiello and co-workers (3,25)). Notably, the intracellular domains, the CT, CL, and NT, which have been implicated in V_j gating, are identical to that of Cx32. It is well established that N2E, T4D, and G5D substitutions reverse the polarity of the V_j gates so that it is opposite to the polarity of loop-gate closure in both macroscopic and single-channel recordings of Cx32 intercellular channels and in macroscopic and single-channel recordings of undocked Cx32*43E1 hemichannels (3,8,11,12). This allows unequivocal discrimination of the two gating mechanisms in the undocked hemichannel. Significantly, because the voltage sensors of both gates respond only to the component of applied voltage that is oriented across the length of the intercellular channel pore (the transjunctional voltage, V_j) and not to changes in absolute membrane potential (V_m), the relevant parameter

is the electric field within or close to the aqueous channel pore. Because the orientation of this field will be the same when voltage is applied to either an intercellular or an undocked hemichannel, the response of undocked hemichannels to voltage will report the operation of the same voltage-dependent gates as that of hemichannels when they are paired to form intercellular channels. For these reasons, comparison of macroscopic recordings of Cx32*43E1 and Cx32*434E1 N2E undocked hemichannels provide an unequivocal means to determine the role of the Cx32 CT in V_j (fast) gating.

We report that both V_j (fast) gates and loop (slow) gates are operational in Cx32*43E1 N2E 219-stop undocked hemichannels.

MATERIALS AND METHODS

Molecular biology

Mutations of Cx32*43E1 were produced with the QuikChange II Site-Directed Mutagenesis Kit (Agilent Technologies, Santa Clara, CA) and sequenced in entirety. Introduction of a stop codon at position 220 results in truncation of the C-terminus at residue 219. The terminal sequence becomes $ACAR^{219}$, which is identical to that described by Revilla et al. (19), although these authors refer to the mutation as the "220 stop". However, their construct did not introduce a stop codon at 220. This may add an additional sequence encoded by the vector to the Cx32 C-terminus (19) after residue 219, following DNA linearization with an unspecified restriction enzyme in the vector linker that precedes in vitro RNA synthesis.

Expression in oocytes

DNA clones were linearized with a unique *Hin*dIII site in the linker of the pGEM 7zf vector (Promega, Madison, WI). RNA was synthesized from this DNA template with the mESSAGE mACHINE T7 promoter kit (Ambion/Life Technologies, Invitrogen, Carlsbad, CA) and purified using a MEGAclear kit (Ambion/Life Technologies, Invitrogen). A quantity of 100 nL of purified RNA (~5 ng/nL) was injected into each *Xenopus* oocyte (*Xenopus*-1, Dexter, MI). Oocytes were cultured in media containing 100 NaCl mM, 1 mM KCl, 1.8 mM $CaCl_2$, 1 mM $MgCl_2$, 0.01 mM EDTA, and 10 mM HEPES, pH 7.6 at 16°C. When necessary, oocytes were preinjected with 30 nL of an antisense phosphorothioate oligonucleotide (0.3 pmol/nL) complimentary to *Xenopus* Cx38 (26,27). This antisense oligonucleotide reduces expression of endogenous Cx38 hemichannel oocyte currents within 24 h. Notably, expression of Cx32*43E 219 stop and Cx32*43E1 N2E 219 stop hemichannels requires injection of large amounts of RNA, and expression is typically observed after 1–3 days, unlike most Cx32*43E1 constructs, which express membrane currents within 12–24 h. The difference in onset of expression may reflect reductions in hemichannel assembly or trafficking as discussed by Revilla et al. (19).

Electrophysiological recording

Methods are described in Tang et al. (28). The bath solution contained 100 mM cesium methanesulfonate, 10 mM HEPES, pH 7.6, and 0, 1.8, and 5 mM $MgCl_2$, as indicated. Deionized water with a resistance of 18 MΩ cm (Milli-Q water; Millipore, Billerica, MA) was used in solution preparation to minimize the presence of contaminating heavy metals. Recording pipette solutions contained 3 M CsCl and 10 mM HEPES, pH 7.6. Pipette resistances were between 0.1 and 0.25 MΩ. A separate ground chamber containing 3 M CsCl was connected to the bath chamber with an agar bridge containing 3 M CsCl. Membrane currents were recorded with a CA-1B high-performance oocyte clamp (Dagan Instruments, Minneapolis, MN) at room temperature. Currents were digitized at a sampling frequency of 5 kHz and filtered at 100 Hz with a low-pass Bessel filter for presentation.

RESULTS AND DISCUSSION

We have previously reported by single-channel and macroscopic recordings of intercellular homotypic and heterotypic channels that negative charge substitutions at the second locus reverse the polarity of the V_j gates of Cx32 hemichannels and its chimera Cx32*43E1 (5,7,11,12). In undocked Cx32*43E1 hemichannels, closure of both V_j (fast) and loop (slow) gates are favored at inside negative potentials (membrane hyperpolarization from 0 mV) and both V_j- and loop-gating events are observed in single-channel recordings at these potentials. The Cx32*434E1 hemichannel resides in the open state, with membrane depolarization more positive than −20 mV (12,28). In Cx32*43E1 N2E hemichannels, the polarity of the V_j gates is reversed such that channel closure is observed at inside positive potentials $\geq$30 mV (membrane depolarization from 0 mV) in single-channel records. The polarity of loop-gate closure is unchanged by the N2E mutation. In macroscopic recordings, loop-gate closure corresponds to current relaxations observed with hyperpolarization more negative than −30 mV. Single-channel studies of undocked Cx32*43E1 N2E hemichannels confirm that these macroscopic current relaxations correspond to V_j (fast)-gating events with depolarization and loop (slow)-gating events with hyperpolarization (12).

Fig. 1 shows macroscopic currents elicited by membrane polarizations of *Xenopus* oocytes expressing Cx32*43E1 219 stop (Fig. 1 *A*) and Cx32*43E1 N2E 219 stop (Fig. 1 *B*) in bath solutions containing 0, 1.8, and 5 mM $MgCl_2$ from a holding potential of 0 mV. The records shown for each mutation were obtained from the same oocyte after exchange of the external bath solution to change $[Mg^{2+}]$. In all cases, oocytes were first recorded in 1.8 mM Mg^{2+} followed by 0 and then 5 mM Mg^{2+}. The results are representative of records obtained for 10 Cx32*43E1 219 stop and >20 Cx32*43E1 N2E 219 stop oocytes, recorded in one or more external Mg^{2+} concentrations.

As expected (Fig. 1 *A*), current relaxations for Cx32*43E1 219 stop hemichannels are only observed with membrane hyperpolarization, consistent with the negative polarity of both V_j (fast) and loop (slow) gates previously reported for full-length Cx32*43E1 undocked hemichannels (12,28). The relative insensitivity of current relaxations at hyperpolarizing potentials in 0 Mg^{2+} (*left panel*) most likely reflects a series-resistance problem resulting from high Cx32*43E1 expression in this oocyte (>20 μA at −100 mV). In oocytes with less expression (<10 μA at −100 mV), current relaxations are substantially more sensitive to voltage with current relaxations evident at

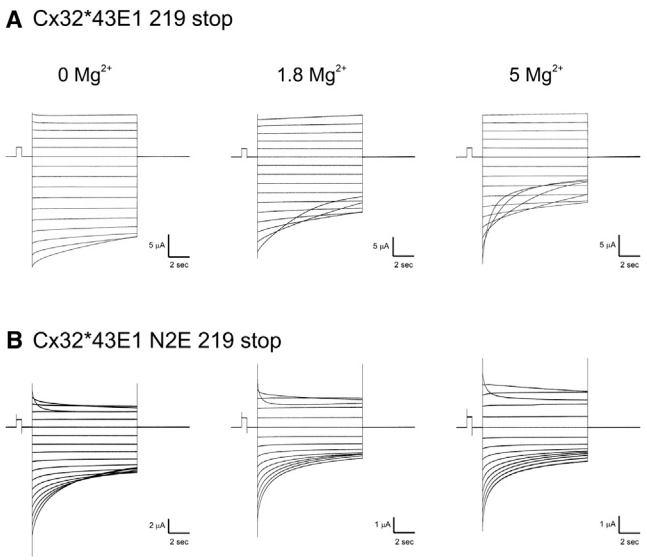

FIGURE 1 Current-voltage relations of Cx32*43E1 hemichannels truncated at residue 219. (*A*) Cx32*43E1 219 stop. Current traces evoked by sequential membrane polarizations ranging from +50 to −100 mV in 10 mV increments from a holding potential of 0 mV. (*B*) Cx32*43E1 N2E 219 stop. Current traces evoked by sequential membrane polarizations in 10 mV increments from a holding potential of 0 mV ranging from +50 to −120 mV. In all cases, currents were normalized to a 500-ms, 10-mV prepulse. The slowing of the time course of current relaxations in Cx32*43E1 N2E 219 stop evoked by hyperpolarization to −80 and −90 mV in 1.8 and 5 mM Mg^{2+} results from the transient activation of an endogenous oocyte current. Transient activation of another endogenous slowly developing outward current is observed in some but not all current traces evoked by depolarization (for example: the current trace evoked by 50 mV in Cx32*43E1 219 stop and by 30 mV in Cx32*43E1 N2E 219 stop in 1.8 Mg^{2+} and the current traces evoked by 30 and 40 mV in 5 mM Mg^{2+}. These endogenous currents are not observed in all oocytes.

voltages more negative than −50 mV (not shown). The increased sensitivity of membrane currents to voltage at higher [Mg^{2+}] is consistent with the reports that divalent cations stabilize the loop-gate closed state but not the V_j-closed state of Cx46 channels (29). A recent report (30) suggests that divalent cations may also destabilize the open state of Cx26 undocked hemichannels. Both stabilization of closed states and/or destabilization of open states by divalent cations will result in faster closing time constants with increasing concentrations of divalent cations.

The relaxation of currents at depolarizing potentials ≥30 mV observed in the records for Cx32*43E1 N2E 219 stop (Fig. 1 *B*) correspond to closure of V_j (fast) gates, as shown previously for full-length Cx32*43E1 N2E undocked hemichannels, indicating that the V_j (fast) gates are operational when the CT is shortened to four residues. Thus, the differences in the voltage-dependences of current relaxations of Cx32*43E1 219 stop and Cx32*43E1 N2E 219 stop at hyperpolarizing (negative) potentials are consistent with the operation of both gates in Cx32*43E1 hemichannels and operation of only the loop gates in Cx32*43E1 N2E hemichannels at hyperpolarizing potentials.

The results shown in Fig. 1 also indicate that the reversal of the polarity of V_j (fast) gates is independent of external [Mg^{2+}] and that loop gating does not arise from Mg^{2+} block, as reported for Cx37 (31). The time constants of current relaxations corresponding to loop gating of Cx32*43E1 N2E hemichannels progressively shorten with increasing [Mg^{2+}]. For example, the macroscopic current relaxation at −70 mV for the oocyte shown in Fig. 2 *B* is well fitted by two exponentials with time constants ~6.46 and 0.83 s (0 Mg^{2+}): 4.19 and 0.55 (1.8 mM Mg^{2+}), and 4.07 and 0.52 (5 mM Mg^{2+}), respectively. The onset of current relaxations also occurs at smaller potentials as [Mg^{2+}] is increased: −40 mV in 0 Mg^{2+} compared to −20 mV in 1.8 and 5 mM Mg^{2+}. Interestingly, the loop gates of Cx32*43E1 N2E hemichannels appear to be less sensitive to extracellular [Mg^{2+}] than are Cx26, Cx46, and Cx38 hemichannels (29,30,32). The relative insensitivity of Cx32*43E1 undocked hemichannels to divalent cations contrasts with that of *Xenopus* Cx38 hemichannels. This differential sensitivity allows confirmation of the absence or low levels of endogenous Cx38 currents in the recordings shown in Fig. 1.

The time constants of current relaxations resulting only from V_j gating at 50 mV in 0 Mg^{2+} for the N2E truncation mutant are similar to those of the full-length N2E channel:

$\tau_1 = 0.73$ s ± 0.24, $\tau_2 = 0.15$ s ± 0.06, $n = 12$; and $\tau_1 = 0.66$ s ± 0.31, $\tau_2 = 0.13$ s ± 0.06, $n = 8$, respectively ($p = 0.56$ for τ_1, Student's two-tailed *t*-test).

Similarly, the time constants at 40 mV for the N2E truncation mutation and full-length N2E channels are:

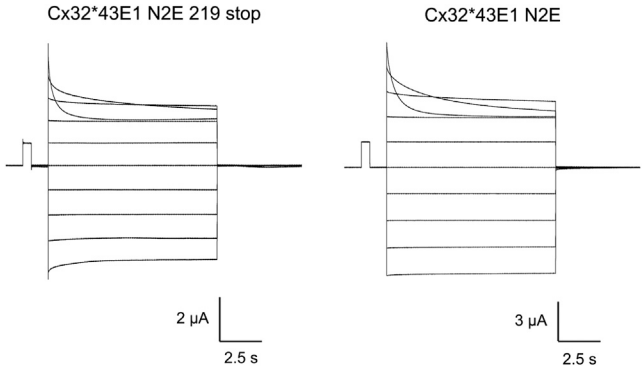

FIGURE 2 Representative current-voltage relations of Cx32*43E1 N2E 219 stop and Cx32*43E1 N2E undocked hemichannels in bath solutions containing 0 Mg^{2+}. Current traces were evoked by sequential membrane polarizations ranging from +50 mV to −40 mV in 10-mV increments from a holding potential of 0 mV and normalized to a 500-ms, 10-mV prepulse. Current relaxations elicited by membrane depolarization to 40 and 50 mV correspond to operation of V_j (fast) gates. The time constants for current relaxations, fitted to two exponentials, are similar for both channels. At 50 mV: $\tau_1 = 0.88$ s and $\tau_2 = 0.19$ s for the 219 stop channel; $\tau_1 = 1.29$ s and $\tau_2 = 0.33$ s for the full-length channel. At 40 mV: $\tau_1 = 4.62$ s and $\tau_2 = 0.35$ s for the 219 stop channel; $\tau_1 = 4.17$ s and $\tau_2 = 0.33$ s for the full-length channel.

$\tau_1 = 3.27$ s $\pm$ 1.44, $\tau_2 = 0.40$ s $\pm$ 0.14, $n = 14$; and $\tau_1 = 3.30$ s $\pm$ 1.28, $\tau_2 = 0.43$ s $\pm$ 0.13, $n = 10$, respectively ($p = 0.96$ for τ_1, Student's two-tailed t-test).

Representative current traces of full-length Cx32*43E1 N2E and Cx32*43E1 N2E 219 stop are shown in Fig. 2. The similarity of time constants suggests that the truncation does not substantially alter the relative free energy difference between the open and V_j-closed state(s) of Cx32*43E1 N2E 291 stop and full-length Cx32*43E1 N2E hemichannels at 40 and 50 mV.

We conclude that CT sequence distal to residue 219 (i.e., residues 220–283) is not required for V_j gating of the Cx32*43E1 219 stop and, by extension, the Cx32 219 stop hemichannels.

It is possible that the Cx32 channel examined by Revilla et al. (19) contains an unspecified number of nonconnexin amino acids added to the CT after residue 219 and that addition of these residues may have altered or prevented the operation of the V_j gate. This possibility arises from the report that addition of GFP to the CT of Cx43 appears to prevent the operation of the V_j (fast) gate of Cx43 hemichannels, presumably by interfering with the ability of the CT to interact with the receptor contained within the CL (4,10). Given that undocked Cx32*43E1 N2E hemichannels truncated at residue 247 also display V_j gating (not shown) and that the CTs of Cx43, Cx26, and Cx32 are largely unstructured (15,24,33), it seems unlikely that the apparent loss of V_j gating reported by Revilla et al. (19) results from the addition of a few nonconnexin residues to the end of residue 219, as these are unlikely to interfere with a possible CT-CL interaction similar to that produced by GFP attachment to the CT of Cx43.

Truncation at residue 219 reduces the length of the CT from 67 to 4 amino acids. The four remaining amino acids could have a maximal length of ~20 Å (4 × 5 Å) in an extended conformation. Based on the Cx26 crystal structure and a homology model of Cx32*43E1 N2E with the CT truncated at 217 (Fig. 3, *A* and *B*), both of which were equilibrated by all-atom molecular dynamics (MD) simulation in a fully hydrated membrane environment, the distance between the end of CT of 219 stop and the intracellular entrance of the channel pore will exceed 20 Å. This indicates that the truncated CT could not cause V_j (fast) gating by either serving as a particle that physically occludes the open channel pore or by interacting with the first 12 residues of the N-terminus when the channel resides in the open state. Recall that the first 12 NT residues reside in the channel pore and may contain at least a part of the V_j-gate voltage sensor. The same argument can be made for the CT of Cx26. Fig. 3, *C* and *D*, shows the average equilibrated structure of the Cx26 hemichannel after equilibration of the Cx26 crystal by all-atom MD. The full-length Cx26 CT is also too short to enter the open channel pore or to interact with the first 12 residues of the N-terminus. Fig. 3, *C* and *D*, shows

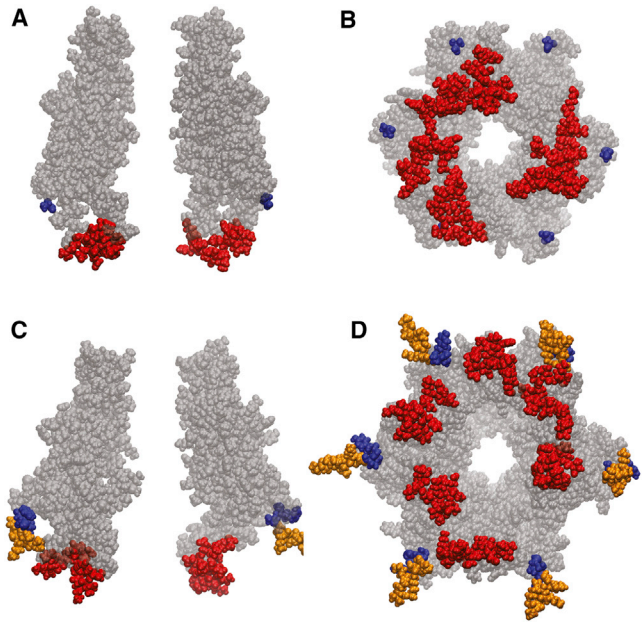

FIGURE 3 Atomic models of the open state of Cx32*43E1 N2E and Cx26 hemichannels after equilibration by all-atom molecular dynamics simulations. (*A*) Side view showing two opposite subunits of Cx32*43E1 N2E residues 1–216. (*B*) Bottom view of six subunits of Cx32*43E1 N2E residues 1–216. (*Red*) Residues 108–122 that correspond to the CL; (*blue*) residue 216. The atomic model was created in the program MODELLER (http://salilab.org/modeller/) using the Cx26 crystal structure as template and equilibrated by all-atom MD simulation in a fully hydrated POPC membrane by the Anton supercomputer (D. E. Shaw Research, New York) for 400 ns. The structure shown is that which corresponds most closely (smallest RMSD) to the average position of all atoms determined for last 100 ns of the MD simulation. We call this the "average equilibrated structure". (*C*) Side view, showing two opposite subunits of Cx26 residues 1–219. (*D*) Bottom view of six subunits of Cx26 residues 1–219. (*Red*) Residues 109–123 are the CL; (*blue*) residues 216–219 correspond to a comparable truncation of the Cx26 CT as examined in this study; (*orange*) residues 220–226 correspond to full-length Cx26.

close proximity between the Cx26 CT and CL in one subunit, but the interaction is not stable, forming and breaking over the course of the MD simulation (T. Kwon and T. A. Bargiello, unpublished).

The computed I-V relation obtained with grand canonical Monte Carlo Brownian dynamics (34,35) of the average equilibrated structure matches experimental single-channel data for both Cx26 (36) and Cx32*43E1 N2E hemichannels (T. Kwon and T. A. Bargiello, unpublished) in symmetric 100 mM KCl. This finding strongly suggests that the structures shown correspond closely to the physiologic open state.

We cannot exclude the possibility that the remaining four residues of the Cx32 CT, $ACAR^{219}$, interact with a region of the CL that is close to the CL/TM3 border. We do not observe connexin hemichannel membrane currents in mutations that further shorten the Cx32*43E1 CT to residue 217 (i.e., 218 stop, not shown). Revilla et al. (19) report the same result for Cx32 intercellular channels. The particle-receptor gating model proposed for Cx43 hemichannels can be

interpreted to suggest that voltage induces conformational changes that include exposure of the L2 receptor in the CL, and that this conformation is stabilized by low-affinity binding of specific sequence contained in the CT (3). If this mechanism is shared by all connexin hemichannels, then the operation of the V_j (fast) gate in the CT truncations of Cx32*43E1 can be explained if the four remaining CT residues ($ACAR^{219}$) are sufficient to interact with a region of the CL near the TM3 border to stabilize the closed conformation. Alternatively, it is possible that the conformation of the Cx32 V_j-closed state is stable in the absence of interactions with the CT and thus, the CT would not be required. Although this appears to be the most likely possibility given the reduced length of the CT and the similarity of the time constant of V_j (fast) gating in the truncated and full-length channels, additional studies are required to determine if the four remaining residues play any role in the operation of the V_j (fast) gate.

CONCLUSIONS

Both V_j (fast) gates and loop (slow) gates operate in a truncation mutation (219 stop), which removes all but four amino acids of the CT of a Cx32 chimeric hemichannel (Cx32*43E1). Thus, residues 220–283 are not required for expression of V_j (fast) gating of Cx32*43E1 undocked hemichannels and by extension from previous studies, also Cx32 hemichannels. The results contrast the conclusion reached by Revilla et al. (19) that the CT of Cx32 distal to residue 219 contains a gating particle that plays an essential role in establishing V_j (fast) gating. If the CT of Cx32 has a direct role in establishing V_j (fast) gating, mediated by an interaction between the CT and CL/TM3, then this interaction must be restricted to the four amino-acid residues ($ACAR^{219}$) that remain after insertion of a stop codon at residue 220.

We thank Drs. Andrew Harris (University of Medicine and Dentistry of New Jersey) and Michael Bennett (Albert Einstein College of Medicine) for comments on the manuscript.

The Cx32*43E1 N2E structural model shown was equilibrated by all-atom MD simulation performed on the Anton supercomputer by grant No. PSCA00045P from the National Resource for Biomedical Supercomputing to T.A.B. This work was supported in part by National Institutes of Health grant No. 1R01GM098584.

REFERENCES

1. Trexler, E. B., M. V. Bennett, …, V. K. Verselis. 1996. Voltage gating and permeation in a gap junction hemichannel. *Proc. Natl. Acad. Sci. USA.* 93:5836–5841.
2. Srinivas, M., J. Kronengold, …, V. K. Verselis. 2005. Correlative studies of gating in Cx46 and Cx50 hemichannels and gap junction channels. *Biophys. J.* 88:1725–1739.
3. Bargiello, T. A., Q. Tang, …, T. Kwon. 2012. Voltage-dependent conformational changes in connexin channels. *Biochim. Biophys. Acta. Biomembr.* 1818:1807–1822.
4. Bukauskas, F. F., and V. K. Verselis. 2004. Gap junction channel gating. *Biochim. Biophys. Acta. Biomembr.* 1662:42–60.
5. Verselis, V. K., C. S. Ginter, and T. A. Bargiello. 1994. Opposite voltage gating polarities of two closely related connexins. *Nature.* 368:348–351.
6. Gonzalez, D., J. M. Gomez-Hernandez, and L. C. Barrio. 2006. Species specificity of mammalian connexin-26 to form open voltage gated hemichannels. *FASEB J.* 20:2329–2338.
7. Oh, S., J. B. Rubin, …, T. A. Bargiello. 1999. Molecular determinants of electrical rectification of single channel conductance in gap junctions formed by connexins 26 and 32. *J. Gen. Physiol.* 114:339–364.
8. Purnick, P. E. M., S. Oh, …, T. A. Bargiello. 2000. Reversal of the gating polarity of gap junctions by negative charge substitutions in the N-terminus of connexin 32. *Biophys. J.* 79:2403–2415.
9. Rackauskas, M., M. M. Kreuzberg, …, F. F. Bukauskas. 2007. Gating properties of heterotypic gap junction channels formed of connexins 40, 43, and 45. *Biophys. J.* 92:1952–1965.
10. Contreras, J. E., J. C. Sáez, …, M. V. L. Bennett. 2003. Gating and regulation of connexin 43 (Cx43) hemichannels. *Proc. Natl. Acad. Sci. USA.* 100:11388–11393.
11. Oh, S., S. Rivkin, …, T. A. Bargiello. 2004. Determinants of gating polarity of a connexin 32 hemichannel. *Biophys. J.* 87:912–928.
12. Oh, S., C. K. Abrams, …, T. A. Bargiello. 2000. Stoichiometry of transjunctional voltage gating polarity reversal by a negative charge substitution in the amino terminus of a connexin32 chimera. *J. Gen. Physiol.* 116:13–31.
13. González, D., J. M. Gómez-Hernández, and L. C. Barrio. 2007. Molecular basis of voltage dependence of connexin channels: an integrative appraisal. *Prog. Biophys. Mol. Biol.* 94:66–106.
14. Oshima, A., K. Tani, …, G. E. Sosinsky. 2007. Three-dimensional structure of a human connexin26 gap junction channel reveals a plug in the vestibule. *Proc. Natl. Acad. Sci. USA.* 104:10034–10039.
15. Maeda, S., S. Nakagawa, …, T. Tsukihara. 2009. Structure of the connexin 26 gap junction channel at 3.5 Å resolution. *Nature.* 458:597–602.
16. Lewandowski, R., J. Shibayama, …, M. Delmar. 2009. Chemical gating of connexin channels. *In* Connexins. A. L. Harris and D. Locke, editors. Humana Press, Totowa, NJ, pp. 129–142.
17. Trexler, E. B., F. F. Bukauskas, …, V. K. Verselis. 1999. Rapid and direct effects of pH on connexins revealed by the connexin46 hemichannel preparation. *J. Gen. Physiol.* 113:721–742.
18. Moreno, A. P., M. Chanson, …, M. Delmar. 2002. Role of the carboxyl terminal of connexin43 in transjunctional fast voltage gating. *Circ. Res.* 90:450–457.
19. Revilla, A., C. Castro, and L. C. Barrio. 1999. Molecular dissection of transjunctional voltage dependence in the connexin-32 and connexin-43 junctions. *Biophys. J.* 77:1374–1383.
20. Seki, A., H. S. Duffy, …, M. Delmar. 2004. Modifications in the biophysical properties of connexin43 channels by a peptide of the cytoplasmic loop region. *Circ. Res.* 95:e22–e28.
21. Shibayama, J., C. Gutiérrez, …, M. Delmar. 2006. Effect of charge substitutions at residue his-142 on voltage gating of connexin43 channels. *Biophys. J.* 91:4054–4063.
22. Hirst-Jensen, B. J., P. Sahoo, …, P. L. Sorgen. 2007. Characterization of the pH-dependent interaction between the gap junction protein connexin43 carboxyl terminus and cytoplasmic loop domains. *J. Biol. Chem.* 282:5801–5813.
23. Shibayama, J., R. Lewandowski, …, M. Delmar. 2006. Identification of a novel peptide that interferes with the chemical regulation of connexin43. *Circ. Res.* 98:1365–1372.
24. Bouvier, D., G. Spagnol, …, P. L. Sorgen. 2009. Characterization of the structure and intermolecular interactions between the connexin40 and connexin43 carboxyl-terminal and cytoplasmic loop domains. *J. Biol. Chem.* 284:34257–34271.
25. Bargiello, T., and P. Brink. 2009. Voltage gating mechanisms of connexin channels. *In* Connexins. A. L. Harris and D. Locke, editors. Humana Press, Totowa, NJ, pp. 103–128.

26. Barrio, L. C., T. Suchyna, …, B. J. Nicholson. 1991. Gap junctions formed by connexins 26 and 32 alone and in combination are differently affected by applied voltage. *Proc. Natl. Acad. Sci. USA.* 88:8410–8414.

27. Rubin, J. B., V. K. Verselis, …, T. A. Bargiello. 1992. Molecular analysis of voltage dependence of heterotypic gap junctions formed by connexins 26 and 32. *Biophys. J.* 62:183–193, discussion 193–195.

28. Tang, Q., T. L. Dowd, …, T. A. Bargiello. 2009. Conformational changes in a pore-forming region underlie voltage-dependent "loop gating" of an unapposed connexin hemichannel. *J. Gen. Physiol.* 133:555–570.

29. Verselis, V. K., and M. Srinivas. 2008. Divalent cations regulate connexin hemichannels by modulating intrinsic voltage-dependent gating. *J. Gen. Physiol.* 132:315–327.

30. Lopez, W., J. Gonzalez, …, J. E. Contreras. 2013. Insights on the mechanisms of Ca^{2+} regulation of connexin26 hemichannels revealed by human pathogenic mutations (D50N/Y). *J. Gen. Physiol.* 142:23–35.

31. Puljung, M. C., V. M. Berthoud, …, D. A. Hanck. 2004. Polyvalent cations constitute the voltage gating particle in human connexin37 hemichannels. *J. Gen. Physiol.* 124:587–603.

32. Ebihara, L. 1996. *Xenopus* connexin38 forms hemi-gap-junctional channels in the nonjunctional plasma membrane of *Xenopus* oocytes. *Biophys. J.* 71:742–748.

33. Stauch, K., F. Kieken, and P. Sorgen. 2012. Characterization of the structure and intermolecular interactions between the connexin 32 carboxyl-terminal domain and the protein partners synapse-associated protein 97 and calmodulin. *J. Biol. Chem.* 287:27771–27788.

34. Im, W., S. Seefeld, and B. Roux. 2000. A grand canonical Monte Carlo-Brownian dynamics algorithm for simulating ion channels. *Biophys. J.* 79:788–801.

35. Egwolf, B., Y. Luo, …, B. Roux. 2010. Ion selectivity of α-hemolysin with β-cyclodextrin adapter. II. Multi-ion effects studied with grand canonical Monte Carlo/Brownian dynamics simulations. *J. Phys. Chem. B.* 114:2901–2909.

36. Kwon, T., A. L. Harris, …, T. A. Bargiello. 2011. Molecular dynamics simulations of the Cx26 hemichannel: evaluation of structural models with Brownian dynamics. *J. Gen. Physiol.* 138:475–493.